European Journal of Chemistry 8 (1) (2017) 85-95

European Journal of Chemistry

Journal webpage: www.eurjchem.com

Synthesis, physicochemical, thermal, fluorescence and catalytic activity studies of novel Mn(II), Co(II), Ni(II) and Cu(II) complexes with tridentate (ONS) Schiff base ligand

Manara Ahmed Ayoub *, Eman Hamed Abd-Elnasser, Mona Abdel-Aziz Ahmed
and Marium Girgis Rizk

Chemistry Department, Faculty of Women for Arts, Science and Education, Ain-Shams University, Cairo, 11757, Egypt

* *Corresponding author at: Chemistry Department, Faculty of Women for Arts, Science and Education, Ain-Shams University, Cairo, 11757, Egypt.*
Tel.: +2.02.01006496983. Fax: +2.02.24157804. E-mail address: manara_2005@yahoo.com (M.A. Ayoub).

ARTICLE INFORMATION

DOI: 10.5155/eurjchem.8.1.85-95.1513

Received: 02 December 2016
Received in revised form: 17 January 2017
Accepted: 21 January 2017
Published online: 31 March 2017
Printed: 31 March 2017

KEYWORDS

ONS donor sites
Catalytic activity
Thermal analysis
Schiff base ligand
Metals complexes
Fluorescence spectra
2-((1-(Thiophen-2-yl)ethylidene)amino)phenol

ABSTRACT

Syntheses and physicochemical studies of Mn(II), Co(II), Ni(II) and Cu(II) complexes with tridentate Schiff base ligand (*E*)-2-((1-(thiophen-2-yl)ethylidene)amino)phenol (HL) (ATS) were characterized by elemental analysis, FT-IR, Mass, ^{1}H NMR, UV-Vis, magnetic moment, thermal analysis (TG and DTG) techniques, molar conductance and fluorescence spectra. The IR spectra showed that complexes were coordinated in metal ions via the imine N, O and S atoms. Magnetic and UV-Vis spectra, indicated that the geometrical structure of Mn(II), Co(II) and Ni(II) complexes are an octahedral while Cu(II) is a tetrahedral. The kinetic thermodynamic parameters such as E^*, ΔH^*, ΔS^* and ΔG^* were determined for each thermal degradation stage of TG curves of the metal(II) complexes using Coat-Redfern method. Fluorescence studies indicated that the Schiff base ligand HL (ATS), and its metal(II) complexes can serve as potential photoactive materials as indicated from their characteristic fluorescence properties and study the effect of solvent and pH on it. The catalytic activities of metal(II) complexes were studied using H_2O_2 solution.

Cite this: *Eur. J. Chem.* **2017**, *8(1)*, 85-95

1. Introduction

Schiff bases have often been used as chelating ligands in coordination chemistry. It is well known that N and S atoms play a key role in the coordination of metals at the active sites of numerous metallobio molecules [1]. Schiff base metal complexes have been widely studied because they have industrial, antifungal, antibacterial, anticancer, anti-oxidative activity, antibiotics, anti-corrosion and catalysis applications [2-4]. The Schiff base metal complexes are also very useful model systems in chelate chemistry. The metal ion in such complexes can be coordinated by the imine nitrogen atom and also by the other active centers present in the molecule. This can lead to many interesting catalytic and potential properties [5-7]. Schiff base compounds often have the property of luminescence, especially, when their complexes have structure of rigidity plane and rich conjugation [8,9]. Many of tridentate Schiff base ligand showed enhanced fluorescence. Moreover, luminescent compounds of Schiff base ligand and its transition metal complexes are attracting much current research interest because of their application including emitting materials for organic light, light materials for photo fluorescent sensors for organic or inorganic analytes [10-12]. The decomposition of hydrogen peroxide has been used as a model reaction for investigation of the catalytic activity of various transition metal complexes [13].

The present study describes the chelation behaviors of Schiff base derived from the condensation of 2-acetylthiophene with to 2-aminophenol towards Mn(II), Co(II), Ni(II) and Cu(II) in molar ratio (1:1) (Ligand: Metal ion). The metal complexes were characterized by elemental analyses, IR, ^{1}H NMR, MS, UV-Vis, TGA, magnetic moment, molar conductance and fluorescence spectra.

2. Experimental

2.1. Materials and reagents

All chemicals were reagent grade quality purchased from commercial sources and used as received. The chemicals used are of the highest purity available.

http://dx.doi.org/10.5155/eurjchem.8.1.85-95.1513

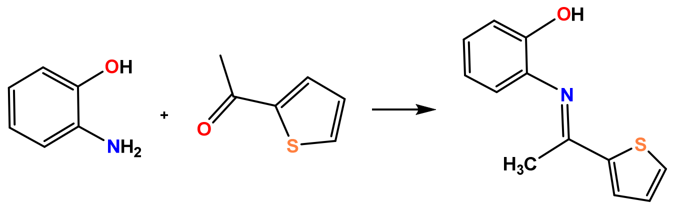

Scheme 1

They include 2-aminophenol (Aldrich), 2-acetylthiophene (Merck), cobalt(II) and nickel(II) chloride hexahydrate and cupper(II) chloride dehydrate and manganese(II) chloride tetrahydrate, organic solvents used are absolute ethanol, methanol, diethyl ether, dimethylformamide (DMF), dimethyl sulfoxide (DMSO), acetonitrile (CH_3CN) and 1,2-dichloro methane as pure grade materials.

2.2. Physical measurements

Elemental analysis (CHNS) was performed on a Perkin Elmer 2400 elemental analyzer. FT-IR measurements (KBr pellets) were carried out on a Shimadzu 8000 FT-IR spectrometer at the central laboratory, Ain Shams University, Egypt. ^{1}H NMR measurements were performed on a Varian-mercury 300 MHz spectrometer at the Microanalytical Center, Cairo University, Giza, Egypt. Samples were dissolved in DMSO-d_6 with TMS as internal reference. Mass spectroscopy measurements of the solid ligands and complexes were carried out on a JEOL JMS-AX500 spectrometer at the National Research Center, Giza, Egypt, magnetic measurements of the complexes were measured by the Gouy method at room temperature using a magnetic susceptibility balance, Sherwood Scientific, Cambridge Science Park, Cambridge England. Thermogravimetric analysis (TG and DTG) were carried out under N_2 atmosphere with a heating rate of 10 °C/min using a Shimadzu DT-50 thermal analyzer at the Microanalytical Center, Cairo University, Giza, Egypt. All conductivity measurements were performed in DMF (1×10^{-3} M) at 25 °C, by using WAP, GMP 50 conductivity meter. Ultraviolet spectra were recorded using a Shimadzu UV 1800 spectrophotometer in the range (200-800 nm) at the Micro analytical Center, Cairo University, Giza, Egypt. The photo luminescent properties of all complexes were studied using a Jenway 6270 fluorimeter, the central laboratory, Ain Shams University, Egypt. All melting points were measured using an ordinary MEL-TEMP II Laboratory device (U.S.A), melting point apparatus.

2.3. Synthesis of the tridentate Schiff base ligand (E)-2-((1-(thiophen-2-yl)ethylidene)amino)phenol Schiff base (HL)

The ligand was synthesized by slow addition of 2-acetylthiophene (1.09 mL, 10 mmole) in 50 mL ethanol to 2-aminophenol (1.09 g, 10 mmole) in 50 mL ethanol. The reaction mixture was heated to reflux for 4 hrs. The dark brown product obtained after cooling was filtered off and washed with different amounts of 1,2-dichloromethane then diethyl ether, fine crystals were obtained by recrystallization from hot ethanol. The reaction for the formation of HL is illustrated in Scheme 1. Yield: 1.645 g, 70%. M.p.: 157-159 °C. FT-IR (KBr, ν, cm^{-1}): 3304 (ν_{OH}, phenolic), 3054 (ν_{C-H}, Ar.), 2958, 2851 ($\nu_{C-H\ asym.\&sym.}$, aliph.), 1602 ($\nu_{C=N}$, azomethine), 1141 (ν_{C-O}, phenolic), 1467 (m) ($\nu_{C=C}$, Ar.), 743 (ν_{C-S}, thiophenolic). MS (EI, *m/z* (%)): 217.10 (M^+, 73.03). ^{1}H NMR (300 MHz, DMSO-d_6, δ, ppm): 3.172 (s, 3H, CH_3), 6.358-6.986 (m, 4H, Ar-H), 7.365-7.722 (m, 3H, thiophene protons), 8.879 (s, 1H, OH). Anal. calcd. for $C_{12}H_{11}NSO$: C, 66.33; H, 5.10; N, 6.45; S, 14.75. Found: C, 66.40; H, 4.87; N, 6.60; S, 14.60%.

2.4. Synthesis of Schiff base metal complexes

A solution of metal salts (1 mmole) in ethanol (50 mL) was added gradually with constant stirring to a solution of ligand HL (1 mmole) in ethanol (50 mL). The solution was refluxed for 2 hrs. On cooling the colored product was precipitated out. It was filtered, and then washed with cold ethanol and diethyl ether.

2.5. The fluorescence spectra of the Schiff bases HL and its metal(II) complexes

The fluorescence spectra of the Schiff bases HL_1 and the metal(II) complexes measured in different solvents, dimethyl formamide (DMF), dimethylsulfoxide (DMSO) and acetonitrile (CH_3CN), in different pH range (2.2-9.4), were recorded at room temperature.

2.6. Catalytic activity of Schiff base ligand HL and its metal(II) complexes

The catalytic activity of the complexes has been evaluated by recording the rate of decomposition of hydrogen peroxide. The weight of metal complex 0.001 g was mixed with 2 mL of H_2O_2 (0.4 %), diluted to 50 mL distilled water and shaking for 10 minutes. After 10 minutes, 5 mL aliquot from the reaction mixture was mixed with 10-15 mL H_2SO_4 (2.0 N) and then titrated against 0.02 M $KMnO_4$, the extent of hydrogen peroxide decomposes at different time (each 5 min; from 0 to 1 hr) were recorded. Repeating with (0.8 and 1.2 %) H_2O_2 with constant weight of metal complexes. A different weight of metal complexes were taken with constant concentration of H_2O_2 (0.4 %).

3. Results and discussion

The analytical and physical data of the Schiff base ligand HL and their metal(II) complexes are listed in Table 1.

3.1. IR spectra of the Schiff base ligands and their metal (II) complexes

The IR spectra of the complexes are compared with those of the free ligand in order to determine the coordination sites that may be involved in chelation, shown in Figure 1 and the assignments are listed in Table 2. Upon comparison, it was determined that the ν(OH) stretching vibration which is found in the free ligand at 3375 cm^{-1} disappeared in the spectra of complex, indicating the participation of OH group in chelate formation. All complexes showed a broad band in the range (3320-3407 cm^{-1}) assigned to ν(OH) of the coordinated or hydrated water molecules associated with the complexes which were confirmed by elemental and thermal analysis. But the participation of the OH group in the complexes were evident from the shift in position of the δ(OH) in plane deformation vibration from 1267 cm^{-1} in the spectrum of the free ligand to (1260-1278 cm^{-1}) range in the spectra of the complexes.

Table 1. Physical and analytical data of the Schiff base, ligand HL and its metal(II) complexes.

Ligand/complex **Molecular formula**	**Yield (%)**	**Color**	**M.p. (°C)**	**Elemental analyses, Found (Calcd.), (%)**			
				C	**H**	**N**	**S**
HL	70	Dark brown	157-159	66.40	4.87	6.60	14.60
$C_{12}H_{11}NOS$				(66.33)	(5.10)	(6.45)	(14.75)
$[Mn(HL)(Cl_2)(H_2O)].3H_2O$	75	Yellow	309-310	34.68	4.62	3.40	7.71
$C_{12}H_{19}NO_5SCl_2Mn$				(34.71)	(4.61)	(3.37)	(7.72)
$[Co(HL)(Cl_2)(H_2O)].5H_2O$	85	Red	315-316	31.64	5.23	3.06	7.03
$C_{12}H_{23}NO_7SCl_2Co$				(31.66)	(5.09)	(3.08)	(7.04)
$[Ni(HL)(H_2O)_2Cl]Cl.4H_2O$	73	Pale brown	322-324	31.66	5.06	3.08	7.03
$C_{12}H_{23}NO_7SCl_2Ni$				(31.68)	(5.10)	(3.08)	(7.05)
$[Cu(HL)(H_2O)]Cl_2.H_2O$	76	Yellowish	320-322	37.17	3.86	3.60	8.25
$C_{12}H_{15}NO_3SCl_2Cu$		brown		(37.17)	(3.90)	(3.61)	(8.27)

Table 2. Characteristic infrared frequencies (cm^{-1}) of the Schiff base ligand HL and its metal(II) complexes *.

Ligand/Complex	$\nu_{OH,}$ **H_2O**	$\nu_{C=N}$	$\nu_{C=C,}$ **Arom.**	ν_{C-O}	ν_{C-S}	ν_{M-N}	ν_{M-O}	ν_{M-S}	ν_{M-Cl}
HL	3375 (v.s)	1602 (s)	1467 (s)	1141 (m)	743 (v.s)	-	-	-	-
$[Mn(HL)(Cl_2)(H_2O)].3H_2O$	3407 (v.s)	1601 (v.s)	1496 (w)	1148 (w)	757 (m)	583 (m)	470 (v.w)	416 (v.w)	410 (w)
$[Co(HL)(Cl_2)(H_2O)].5H_2O$	3383 (v.s)	1591 (v.s)	1461 (w)	1175 (w)	755 (m)	584 (m)	490 (v.w)	420 (v.w)	418 (w)
$[Ni(HL)(H_2O)_2Cl]Cl.4H_2O$	3382 (v.s)	1604 (s)	1462 (s)	1191 (w)	750 (s)	585 (w)	442 (w)	415 (v.w)	412 (w)
$[Cu(HL)(H_2O)]Cl_2.H_2O$	3320 (m)	1590 (v.s)	1486 (w)	1147 (w)	760 (m)	582 (w)	450 (w)	414 (w)	409 (v.w)

* s, strong; m, medium; br, broad; w, weak.

Additionally the IR spectrum of the ligand HL exhibits medium band at 1141 cm^{-1} which may be referred to ν(C-O) (phenolic) and shifted toward higher frequency in the metal complexes. This shift confirms the participation of the phenolic oxygen in coordination to the metal cation. The IR spectra of the free ligand showed a strong band at 1602 cm^{-1} which is characteristic of the azomethine group. Coordination of the Schiff base to the metal ion through the nitrogen atom is expected to reduce the electron density and so the azomethine frequency shows a decrease in the stretching frequency for the complexes **1**, **2**, **4**, increase in stretching frequency in complex **3**, and being shifted to around (1590-1604 cm^{-1}), which indicates the coordination of the azomethine nitrogen [14]. The strong to medium bands due to ν(C-S) stretching vibration of acetyl thiophene ring appeared at 743 cm^{-1} in the free Schiff base ligand [15,16]. These bands are shifted to 757, 755, 750 and 760 cm^{-1} in Mn(II), Co(II), Ni(II) and Cu(II) metal complexes. These shifts refer to the coordination through acetyl thiophene ring sulfur. The various absorption bands in the region (1461-1496 cm^{-1}) may be assigned due to ν(C=C) aromatic stretching vibrations of 2-acetylthiophene and 2-aminophenol. Conclusive evidence of the banding is also shown by observation that new bands in the spectra of all metal complexes appear in low frequency regions (582-585, 442-490, 414-420 and 409-418 cm^{-1}) characteristic to ν_{M-N}, ν_{M-O}, ν_{M-S} and $\nu_{M-Cl.}$ Finally the results of IR spectra of complexes with ligand HL showed that the ligand behave as monobasic ONS tridentate, bonding to the metal(II) ion through phenolic oxygen, azomethine nitrogen and acetylthiophene ring sulfur.

3.2. Mass spectra

Mass spectrometry has been successfully used to confirm the molecular ion peaks of HL Schiff base and investigate the fragment species. The fragment pattern of mass spectrum gives an impression for the successive degradation of the target compound with the series of peaks corresponding to various fragments. Also, the peaks intensity gives an idea about the stability of fragments especially with the base peak.

The recorded mass spectrum of HL Schiff base ligand confirms the proposed formula of ligand by showing a peak at 217.10 *m/z* due to molecular ion (parent peak) and peak at 218 *m/z* due to (M+1). The series of peaks 57 (100%), 69 (65.17%), 76 (12.36%), 82 (12.36%), 94 (60.67%), 107 (76.40%), 134 (61.80%), 175 (64.04%), 187 (60.67%) and 202 (65.17%) *m/z* may correspond to various fragments and their intensity gives an idea of the stability. The mass fragmentation pattern of HL Schiff base ligand is depicted in Scheme 2.

The mass spectrum of Ni(II) complex $[Ni(HL_1)(H_2O)_2Cl]Cl. 4H_2O$ confirms the proposed formula of the complex by showing a peak at 456 *m/z* due to M+1 and base peak at 353 *m/z.* The series of peaks at 59(21%), 75(15%), 91(32%), 138 (65%), 151 (38%), 153 (41%), 163 (58%), 167 (67%), 175 (65%), 177 (71%), 183 (22%), 191(54%), 276 (16%), 349 (29%) and 353(100%) *m/z* may correspond to various fragments and their intensities which give an idea of their stability Scheme 3.

3.3. ^1H NMR spectral studies

^1H NMR spectrum of the Schiff base ligand, HL was recorded in DMSO-d_6 solution using tetramethylsilane (TMS) as internal standard. The signal at δ 3.172 ppm is assigned to methyl proton. The signals in the range (δ 6.358-7.722 ppm) are assigned to aromatic protons of phenolic and acetyl thiophene ring. The signal at δ 8.879 ppm is assigned to OH proton.

The spectrum of $[Ni(HL)(H_2O)_2Cl]Cl. 4H_2O$ complex showed a singlet signal at δ 3.297 ppm, which has been assigned to methyl protons and shifted to downfield. The signals in the range (δ 6.213-7.679 ppm) were assigned to aromatic protons of phenolic and acetyl thiophene ring sulfur and shifted to upper-field due to increased conjugation on coordination**.** The signal due to OH proton is shifted downfield at δ 9.125 ppm, indicating that OH group is involved in chelation.

3.4. Electronic spectra, magnetic and molar conductance.

The electronic spectrum of the free ligand HL solution in DMF were characterized mainly by two absorption bands. The first absorption band appeared at 266 nm, was assigned to π-π* electronic transitions of phenolic, thiophene ring and azomethine group. The second band appeared at 416 nm was assigned to n-π* transition of the lone pair of oxygen in phenolic, nitrogen in azomethine and sulfur in thiophene ring. In metal complexes, these transitions were found to be shifted to lower or higher energy region compared to the free ligands transition suggesting the coordination of oxygen, nitrogen and sulfur atoms of the ligand to metal (II) ions. The complexes showed additional absorption bands in the range 434-437 nm which could be due to charge transfer transitions and the other types of bands in the visible region in the range 502-762 nm can be attributed to *d-d* transition [17]. Spectral data Table 3, includes electronic spectral studies magnetic moments and molar conductance of Schiff base HL_1 and their metal(II) complexes.

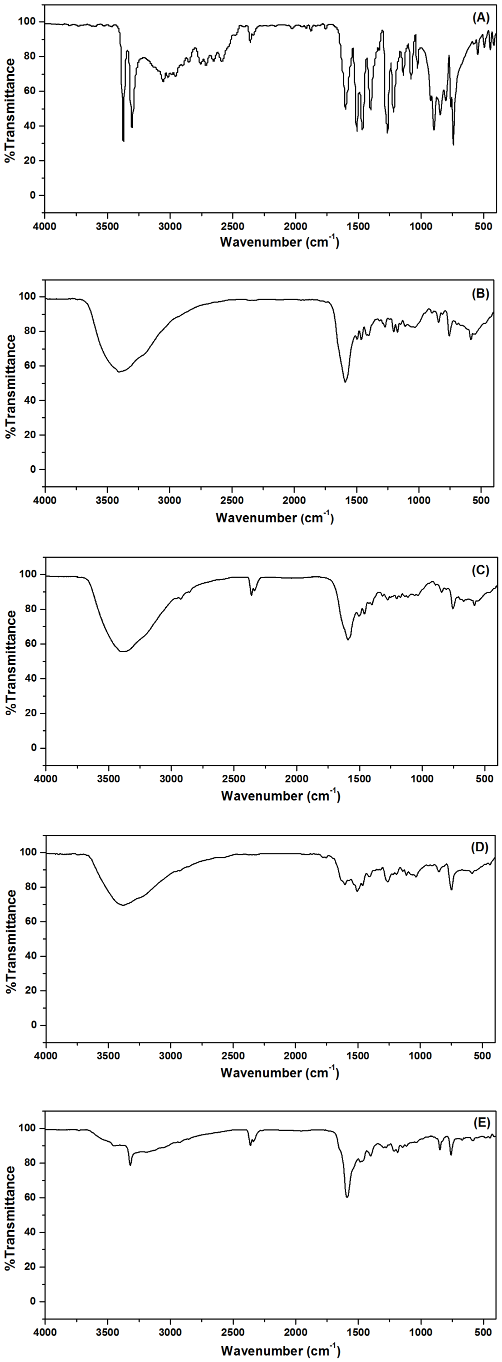

Figure 1. Infrared spectra of (A) the Schiff base ligand, HL; (B) [Mn(HL)(Cl)$_2$(H$_2$O)].3H$_2$O; (C) [Co(HL)(Cl)$_2$(H$_2$O)].5H$_2$O; (D)[Ni(HL)(H$_2$O)$_2$Cl] Cl.4H$_2$O and (E) [Cu(HL)(H$_2$O)]Cl$_2$.H$_2$O.

The Mn(II) complex showed three absorption bands at 714 nm expected for $^4T_{1g}(s)\rightarrow{}^6A_{1g}$, at 610 nm corresponding to $^4T_{2g}(G)\rightarrow{}^6A_{1g}$ and a broad band at 502 nm may be due to $^4T_{1g}(D)\rightarrow{}^6A_{1g}$, and metal to ligand, (MLCT) transitions also occur at 437 nm suggesting an octahedral geometry [18]. The magnetic moment of the Mn(II) complex found to be 5.86 B.M, falls within the range expected for an octahedral geometry.

The electronic spectrum of cobalt (II) complex displays bands at 762, 690 and 503 nm these bands may be assigned to the following transitions $^4T_{1g}(F)\rightarrow{}^4T_{2g}(F)$ ν_1, $^4T_{1g}(F)\rightarrow{}^4A_{2g}(F)$ ν_2 and $^4T_{1g}(F)\rightarrow{}^4T_{1g}(P)$ ν_3, respectively. Suggest an octahedral geometry of Co(II) complex. The magnetic moment of Co(II) complex is found to be 5.82 B.M. Falls within the range expected for octahedral geometry [19].

The electronic spectrum of the Ni(II) complex showed three bands at 729, 682 and 508 nm were assigned to $^3A_{2g}(F)\rightarrow{}^3T_{2g}(F)$, $^3A_{2g}(F)\rightarrow{}^3T_{1g}(F)$ and $^3A_{2g}(F)\rightarrow{}^3T_{1g}(P)$ transitions respectively and metal to ligand charge transfer (MLCT) transition also occur at 434 nm, indicating an octahedral geometry around Ni(II) ion. The magnetic moment of Ni(II) complex is 4.31 B.M an additional evidence for an octahedral complex.

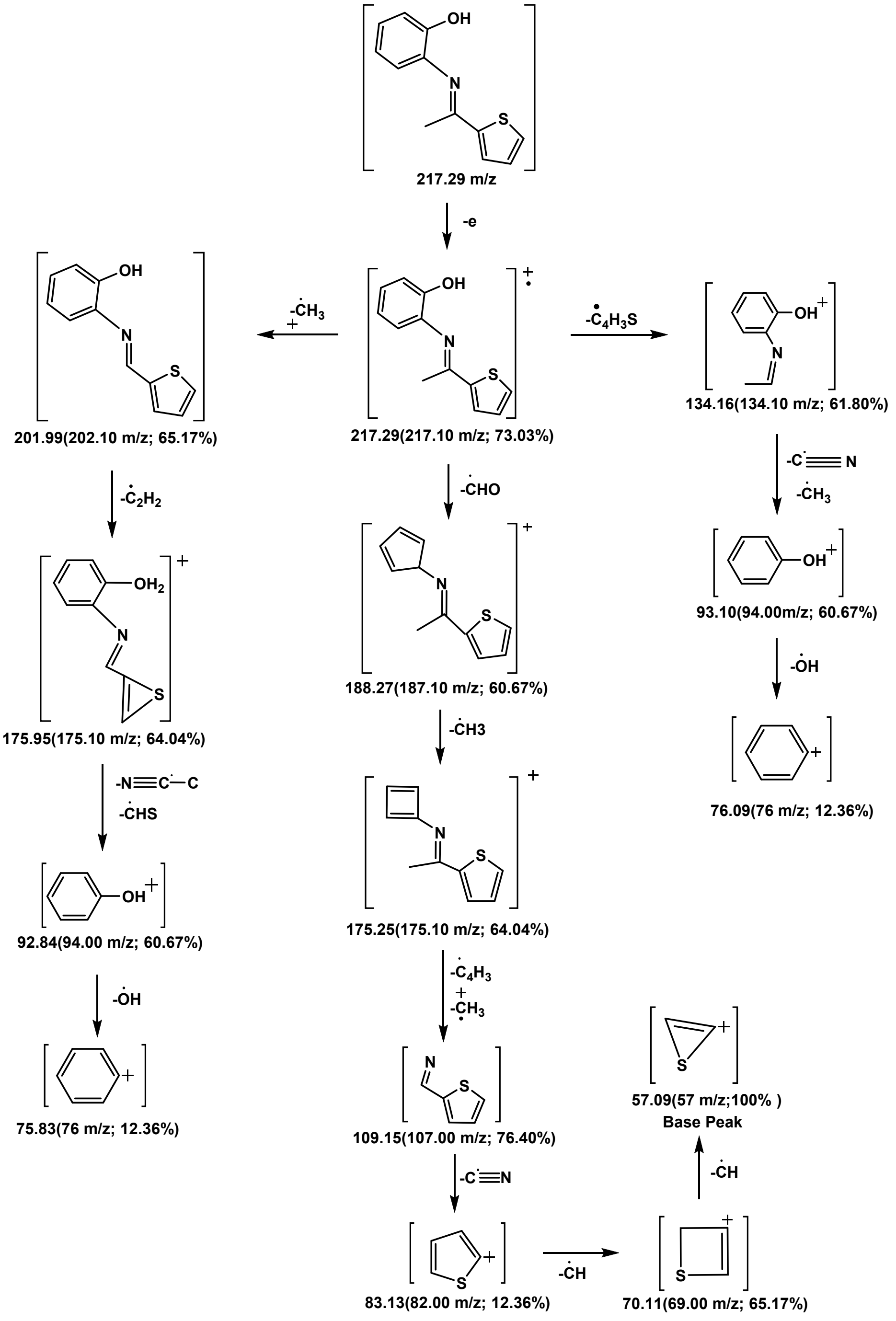

Calculated (Found; Intensity %)

Scheme 2

The electronic spectrum of Cu(II) complex showed band at 729 nm which can be assigned to $^2T_{2g}\rightarrow{}^2Eg$ transition within tetrahedral structure. Also, the spectrum of Cu(II) complex showed band at 435 nm which is assigned to (M→L, CT transition). The magnetic moment of Cu(II) complex was found to be 1.73 B.M, which is close to spin only value.

Molar conductance of the metal(II) complexes are measured in DMF at a concentration of 10^{-3} M. The observed conductance value for Ni(II) complex is 83 ohm^{-1}cm^{2}mol^{-1}, indicates that this complex is (1:1) electrolyte whereas the observed conductance values for Mn(II) and Co(II) complexes are 39.50 and 14.75 ohm^{-1}cm^{2}mol^{-1} which indicates that these complexes are non-electrolytes. But the observed conductance value of Cu(II) complex is 180 ohm^{-1}cm^{2}mol^{-1} indicates that this complex is (1:2) electrolyte.

3.5. Thermal studies

Thermogravimetric (TGA) is a technique in which the change in the weight of a substance is recorded as a function of temperature or time. The TGA curves of the metal complexes is shown in Figure 2 and listed in Table 4.

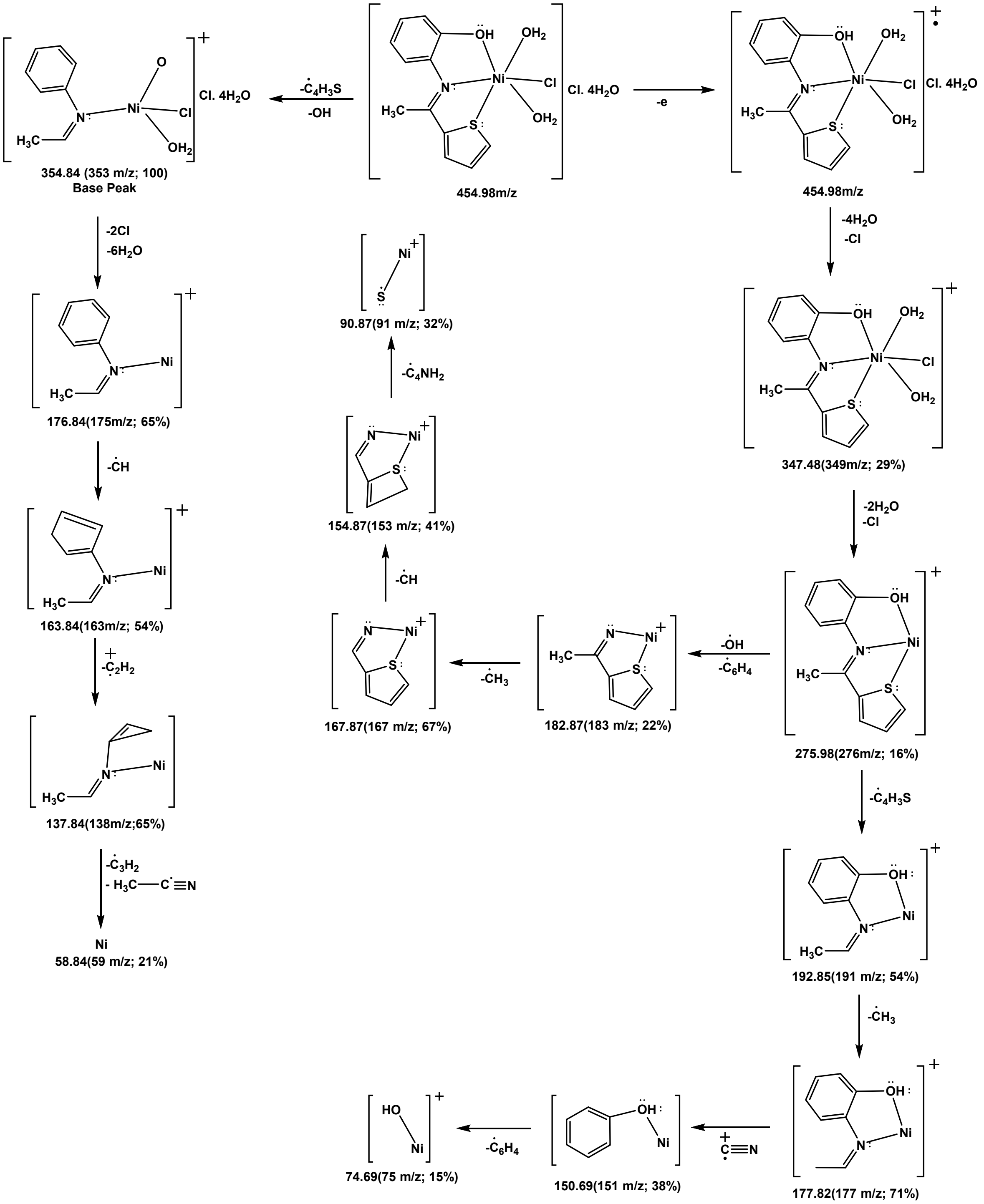

Calculated (Found; Intensity %)

Scheme 3

The thermogravimetric analysis of $[Co(HL)(Cl_2)(H_2O)].5H_2O$ involves three decomposition steps. The first step from 29-103 °C showed removal of the four lattice water with an estimated mass loss of 15.923 (Calc., 15.834%). The second step from 103-309 °C showed loss of one lattice water then coordinated water and removal of $1/2Cl_2$ with an estimated mass loss of 19.139 (Calc., 18.660 %). The last step from 309-1000 °C corresponds to the loss of loss of HCl, C_2H_2, C_3H_4, HCN and H_2 with an estimated mass loss of 42.379 (Calc., 42.423 %). The total mass loss of the decomposition steps is found to be 76.441 (Calc., 76.917%).

The thermogravimetric analysis of $[Ni(HL)(H_2O)_2Cl]Cl.4H_2O$ involves five decomposition steps. The first step from 36-103 °C showed removal of the three lattice water with an estimated mass loss of 12.395 (Calc., 11.882 %).

Table 3. Electronic Spectral data (nm) and magnetic moments of Schiff base HL and their metal(II) complexes.

Compound	$\pi \rightarrow \pi^*$ (nm)	$n \rightarrow \pi^*$ (nm)	Charge transfer (nm)	d -d Transition (nm)	Magnetic moment (B.M.)	Molar conductance $\Omega^{-1}mol^{-1}cm^{-1}$
HL	266	416	-	-	-	-
$[Mn(HL)(Cl_2)(H_2O)].3H_2O$	273	418	437	502, 610,714	5.86	39.50
$[Co(HL)(Cl_2)(H_2O)].5H_2O$	277	412	436	503, 690,762	5.82	14.75
$[Ni(HL)(H_2O)_2Cl]Cl.4H_2O$	275	414	434	508, 682,729	4.31	83
$[Cu(HL)(H_2O)]Cl_2.H_2O$	262	415	435	729	1.73	180

Table 4. Thermoanalytical results (TGA, DTG) of Co(II), Cu(II)and Ni(II) metal complexes with HL.

Complex	Steps	Temperature range (°C)	DTG Peak	TG weight loss, %		Assignment
				Calcd.	Found	
$[Co(HL)(Cl)_2(H_2O)].5H_2O$	1st	29-103	64	15.834	15.923	Loss of four lattice water
	2nd	103-309	219	18.660	19.139	Loss of $2H_2O$, $1/2Cl_2$
	3rd	309-1000	467	42.423	42.379	Loss of HCl, C_2H_2, C_3H_4, HCN, H_2
$[Ni(HL)(H_2O)_2Cl]Cl.4H_2O$	1st	36-103	72	11.882	12.395	Loss of three lattice water.
	2nd	103-203	161	13.349	12.669	Loss of H_2O, $1/2Cl_2$
	3rd	203-296	252	10.206	9.790	Loss of $1/2Cl_2$
	4th	296-445	315	8.348	7.463	Loss of C_2H_2.
	5th	446-1000	563	36.413	37.049	Loss of $2H_2O$, COH, C=N, CH
$[Cu(HL)(H_2O)]Cl_2.H_2O$	1st	37-133	75	4.647	5.184	Loss of one lattice water
	2nd	133-244	204	10.407	10.956	Loss of HCl, H_2
	3rd	244-513	439	31.857	31.708	Loss of $1/2Cl_2$, H_2O, C_3H_3, OH
	4th	513-1000	622	36.818	36.487	Loss of C=N, CH, C-S

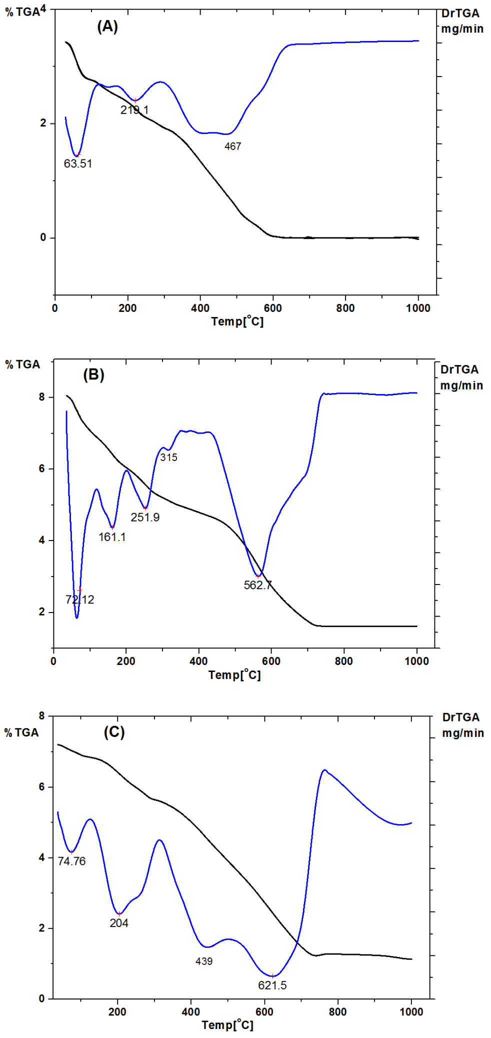

Figure 2. TGA/DTG curves of (A) $[Co(HL)(Cl)_2(H_2O)].5H_2O$; (B) $Ni(HL)(H_2O)_2Cl]Cl.4H_2O$ and (C) $[Cu(HL)(H_2O)]Cl_2.H_2O$.

The second step from 103-203 °C showed removal of one lattice water and $1/2Cl_2$ with an estimated mass loss of 12.669 (Calc., 13.349%). The third step from 203-296 °C corresponds to the loss of $1/2Cl_2$ with an estimated mass loss of 9.790 (Calc., 10.206%). The fourth step from 296-445 °C corresponds to the loss of C_2H_2 with an estimated mass loss of 7.463 (Calc., 8.348%). The last step from 445-1000 °C corresponds to the loss of two coordinated water molecules, COH, C=N, C-H with an estimated mass loss of 37.049 (Calc., 36.412%). The total mass loss of the decomposition steps is found to be 79.366 (Calc., 80.198%).

The thermogravimetric analysis of $[Cu(HL)(H_2O)]Cl_2.H_2O$ involves four decomposition steps. The first step from 37-133 °C showed removal of the one lattice water with an estimated mass loss of 5.184 (Calc., 4.647%). The second step from 133-244 °C showed removal of HCl and H_2 with an estimated mass loss of 10.956 (Calc., 10.407%). The third step from 244-513 °C corresponds to the loss of $1/2Cl_2$, one coordinated water molecule, C_3H_3 and OH with an estimated mass loss of 31.708 (Calc., 31.857%). The last step from 513-1000 °C corresponds to the loss of C=N, CH and C-S with an estimated mass loss of 36.487 (Calc., 36.818 %). The total mass loss of the decomposition steps is found to be 84.335 (Calc., 83.729 %).

3.6. Kinetic data

The kinetic and thermodynamic activation parameters of decomposition processes of complexes namely activation energy (ΔE^*), enthalpy of activation (ΔH^*), entropy (ΔS^*) and Gibbs free energy change of the decomposition (ΔG^*) were evaluated graphically by employing the Coats-Redfern relation [20].

$$\text{Log}\,[\log\{W_f/(W_f - W)\}/T^2] = \text{Log}[AR/q\theta E^*(1-2RT/E^*)] - E^*/2.303RT \quad (1)$$

where E^*, R, A and θ are the heat of activation, the universal gas constant, pre-exponential factor and rate of heating respectively, W_f is the mass loss at the completion of the decomposition reaction, W is the mass loss up to temperature T. Since $1\text{-}2RT/E^* \sim 1$, the plot of the left hand side of equation (1) against 1/T would give a straight line. The other kinetic parameters; the entropy of activation (ΔS^*), enthalpy of activation (ΔH^*) and the free energy change of activation (ΔG^*) were calculated using the following equations:

$$\Delta S^* = 2.303(\log\,(Ah/KT))R \quad (2)$$

$$\Delta H^* = E^* - RT \quad (3)$$

Table 5. The kinetic and thermodynamic data of the thermal decompositions of complexes.

Complex	Stage	Mid Temp. (°K)	ΔE* (KJ/mol)	ΔA (S^{-1})	ΔS* (KJ/mol K)	ΔH* (KJ/mol)	ΔG* (KJ mol)
$[Co(HL)(Cl)_2(H_2O)].5H_2O$	1st	302 - 375	213.55	4.38×10^{-1}	-180.59	2.01	31.151
	2nd	376 - 582	237.29	2.84×10^{-2}	-234.04	2.18	75.172
	3rd	584 - 1273	384.11	1.20×10^{-2}	-268.58	3.73	96.213
$[Ni(HL)(H_2O)_2Cl]Cl.4H_2O$	1st	309 - 376	377.81	3.28×10^{2}	-126.48	4.73	45.273
	2nd	376 - 569	847.05	1.13×10^{-6}	-353.71	7.13	64.216
	3rd	569 - 1273	945.27	8.52×10^{-5}	-378.17	9.84	84.729
$[Cu(HL)(H_2O)]Cl_2.H_2O$	1st	310 - 406	133.84	1.1×10^{-6}	-76.676	0.87	17.154
	2nd	406 - 517	263.57	2.22×10^{-1}	-152.197	0.91	22.712
	3rd	517- 606	369.32	1.33×10^{-1}	-207.765	0.99	77.465
	4th	606 - 1273	429.54	8.97×10^{8}	-287.799	1.26	95.928

Table 6. Fluorescence data of the Schiff base ligand HL and its transition metal (II) complexes.

Name of compound	$\lambda_{excitation}$ (nm)	$\lambda_{emission}$ (nm)
HL	432	604
$[Mn(HL)(Cl)_2(H_2O)].3H_2O$	434	555
$[Co(HL)Cl_2(H_2O)].5H_2O$	436	560
$[Ni(HL)Cl(H_2O)_2]Cl.4H_2O$	434	555
$[Cu(HL)(H_2O)]Cl_2.H_2O$	430	521

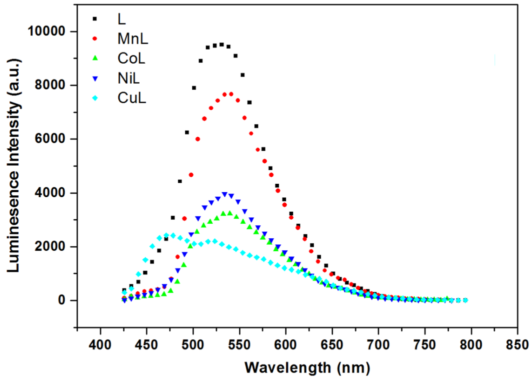

Figure 3. Emission spectra of: (■) Ligand (HL); (●) $[Mn(HL)(Cl)_2(H_2O)].3H_2O$; (▲) $[Co(HL)Cl_2(H_2O)].5H_2O$; (▼) $[Ni(HL)(H_2O)_2Cl]Cl.4H_2O$; and (◆) $[Cu(HL)(H_2O)_2]Cl_2.H_2O$.

$$\Delta G^{*} = H^{*} - T\Delta S^{*} \quad (4)$$

where, (k) and (h) are the Boltzman and Planck constants, respectively. The kinetic parameters are listed in Table 5. From the obtained results, it is apparent that Δ*G** values of the complexes acquire highly positive magnitudes. The high value of the energy of activation of the complexes revealed the high stability of the investigated complexes due to their covalent character [21]. The negative values of Δ*S** for the degradation process indicates that more ordered activated complex than the reactants and the decomposition reaction is slow [22]. The positive values of Δ*H** mean that the decomposition process are endothermic.

3.7. Fluorescence spectral studies

The fluorescence properties of the Schiff base ligand HL and its metal(II) complexes measured in DMSO were recorded at room temperature Figure 3. The excitation spectra of the ligand showed a maximum emission peak at 604 nm when excited at 432 nm. Generally, Schiff base systems exhibits fluorescence due to intra-ligand π-π* transitions. The fluorescent data are summarized in Table 6. The excitation spectrum of Mn(II), Co(II), Cu(II) and Ni(II) complexes exhibited weak fluorescence emission bands in the range 521-560 nm when excited at 430-436 nm range. Significant difference in the position of maximum emission of Schiff base and each metal(II) complexes which is due to the coordination of the metal(II) ion to the ligand. Quenching of fluorescence through complexation is much interesting as it opens up the opportunity for photochemical applications of these complexes [23-25].

3.7.1. Effect of solvent and pH

The influence of the solvent on Schiff base ligand HL and its metal(II) complexes were studied. The results showed that the optimal solvent for Schiff base ligand HL, Mn(II) and Co(II) complexes were DMF at λ_{emi} = 432, 434 and 436 nm, while the optimal solvent for Cu(II) complex was CH_3CN λ_{emi} = 430 nm, as shown in Figure 4. The effect pH on the fluorescence intensity of Schiff base ligand HL and its metal(II) complexes were investigated between the pH range of 2.0-10.0. The influence of pH on Schiff base ligand HL, Mn(II), Co(II) and Cu(II) complex were investigated in both acidic and alkaline media by the addition of dilute HCl and NH_4OH. The optimum signals were recorded in strongly alkaline conditions. The highest intensity of Schiff base ligand HL_1, Mn(II), Co(II) and Cu(II) complexes at 604, 555, 560 and 521 nm were obtained at pH = 9.4, as shown in Figure 4.

3.8. Catalytic Activity

3.8.1. Influence of hydrogen peroxide concentration on the rate of decomposition of Schiff base HL complexes

A definite amount of catalyst (1 mg) was subjected to decomposition reaction by varying the concentration of H_2O_2 (0.4 % to 1.2 %).

Table 7. Influence of H_2O_2 concentration on the rate of decomposition in Schiff base HL complexes.

Amount of catalyst (1 mg)	**Rate constant 10^3 K/min**			
Concentration of H_2O_2	**Mn(II)**	**Co(II)**	**Ni(II)**	**Cu(II)**
0.4%	25.356	31.321	25.333	33.439
0.8%	32.012	35.167	36.341	39.852
1.2%	39.151	44.356	52.462	45.369

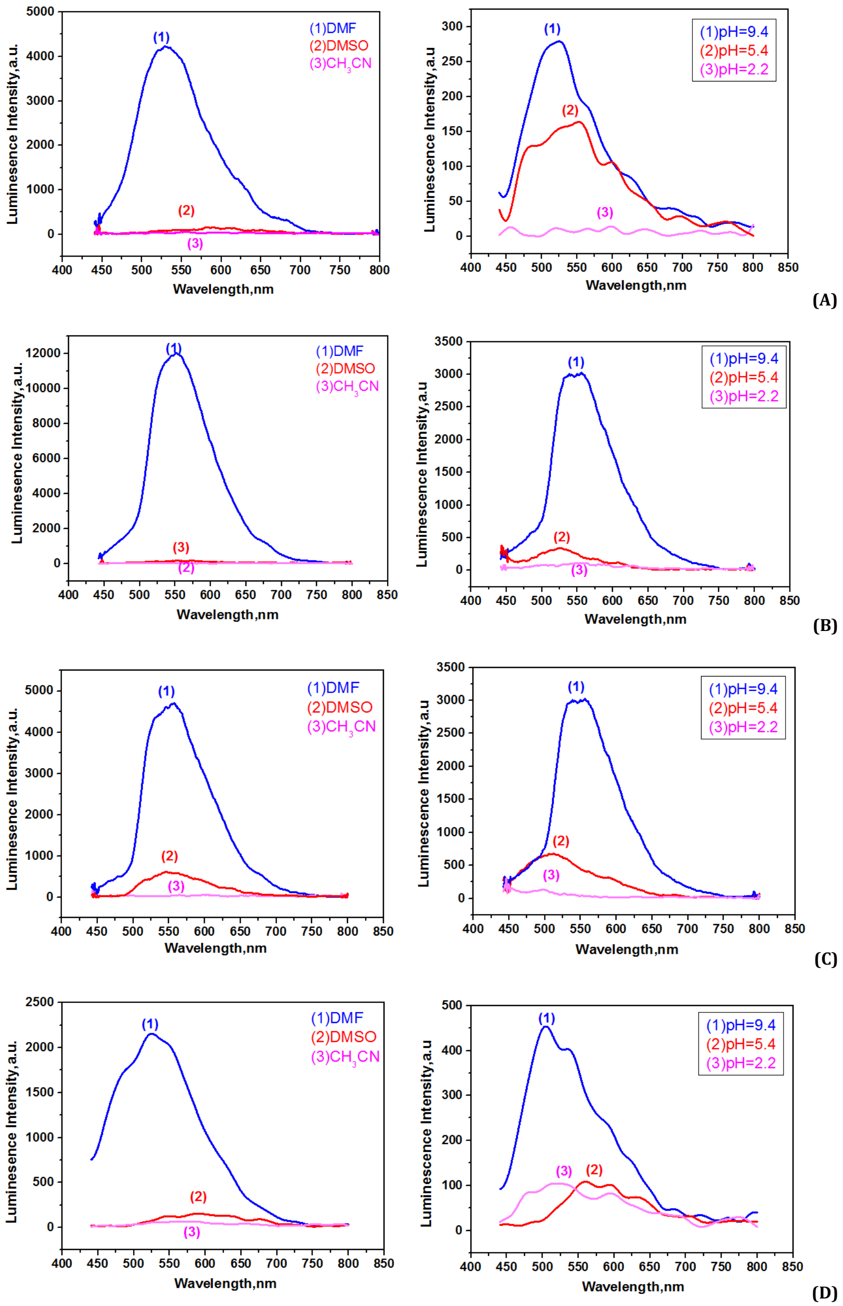

Figure 4. Effect of solvent and pH on (A) Schiff base ligand HL; (B) $[Mn(HL)(Cl)_2(H_2O)].3H_2O$; (C) $[Co(HL)(Cl)_2(H_2O)].5H_2O$ and (D) $[Cu(HL)(H_2O)]Cl_2.H_2O$.

The result for different complexes is given in Table 7 and Figure 5. The rate of reaction is found to increase with increase in concentration of H_2O_2 in all complexes. In case of concentration of H_2O_2 (0.4 and 0.8%) the Cu(II) complex is the most active, while in case of concentration (1.2%) the Ni(II) complex is the most active one.

3.8.2. The Influence of varying amount of catalyst in the Schiff base HL complexes

The effect of varying amount of the catalyst on the decomposition reaction shows first order dependence. For a definite concentration of H_2O_2 (0.4%), varying amounts of catalyst (1 and 3 mg) are subjected to decomposition reaction.

Table 8. The effect of different amounts of catalyst on the decomposition reaction for definite concentration of H_2O_2.

Concentration of H_2O_2 (0.4%)	**Rate constant 10^3 K/min**			
Amount of catalyst (mg)	**Mn(II)**	**Co(II)**	**Ni(II)**	**Cu(II)**
1	25.356	31.321	25.333	33.439
3	111.925	33.669	50.367	53.107

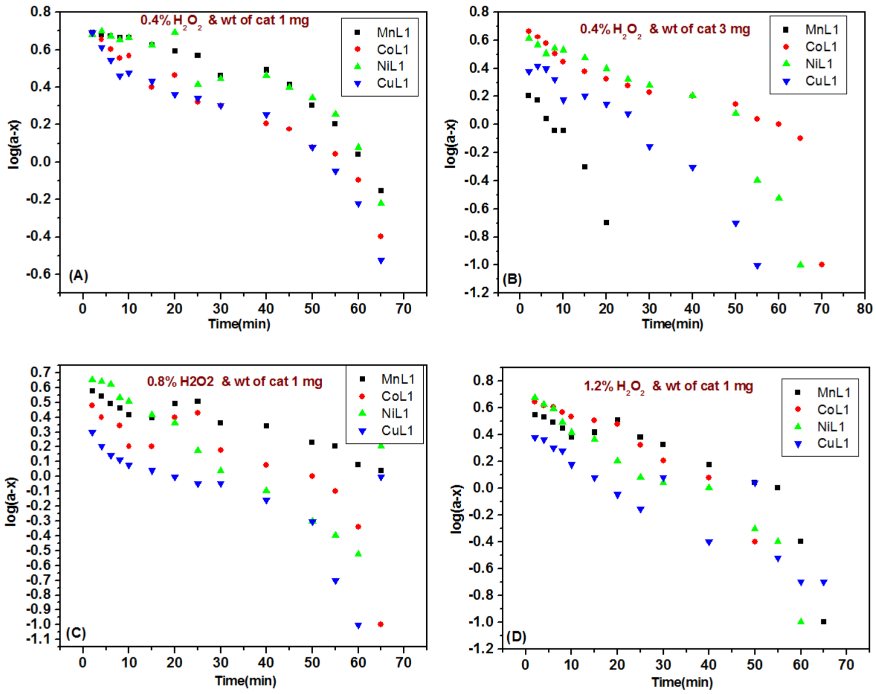

Figure 5. Kinetics of decomposition of hydrogen peroxide concentration (A) 0.4%, wt of catalyst 1 mg; (B) 0.4%, wt of catalyst 3 mg; (C) 0.8%, weight of catalyst 1 mg; (D) 1.2%, weight of catalyst 1mg catalyzed by $[Mn(HL)(Cl)_2(H_2O)].3H_2O$, $[Co(HL)(Cl)_2(H_2O)].5H_2O$, $[Ni(HL)(H_2O)_2Cl]Cl.4H_2O$ and $[Cu(HL)(H_2O)]Cl_2.H_2O$ complexes.

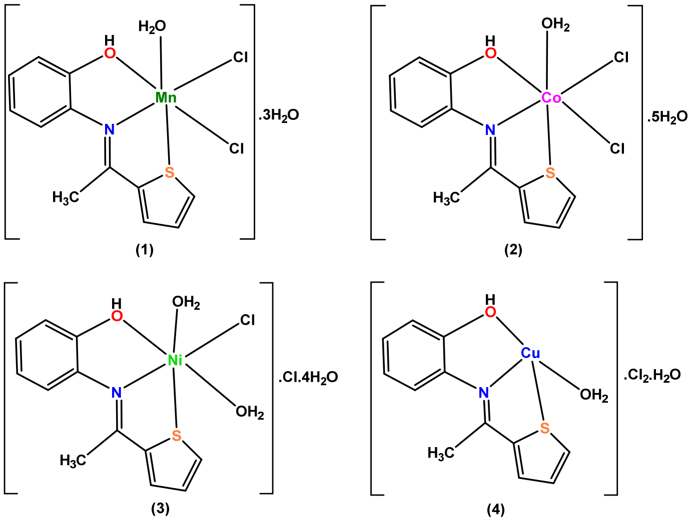

Scheme 4

The rate of the reaction increased with increasing the amount of catalyst. The values are given in Table 8 and Figure 5. Here in case of 1 mg of catalyst, the Cu(II) complex is found to be the most active but in case of 3 mg of catalyst Mn(II) is the most active one.

4. Conclusion

The Schiff base HL ligand and its metal complexes of Mn(II), Co(II) and Ni(II) have been structurally characterized. The spectral data shows that the Schiff base HL ligand acts as tridentate coordinating through phenolic oxygen, azomethine nitrogen and acetylthiophene sulfur.

The analytical, spectroscopic, thermal and magnetic data enable us to predict the possible structures as shown in Scheme 4. In general, all the synthesized compounds can serve as potential photoactive materials, as indicated from their characteristic fluorescence properties. Based on these facts, it could be proposed that these novel materials can be better accommodated for optical applications. The catalytic activities of all Schiff base comp-lexes were studied using H_2O_2 solution. In case of varying concentration of H_2O_2, the catalytic activity increases by increasing the concentration of H_2O_2. The catalytic activity of the complexes was also checked by varying the amount of catalyst. Here also the catalytic activity increases by increasing the amount of catalyst.

References

[1]. Singh, K.; Barwa, M. S.; Tyagi, P. *Eur. J. Med. Chem.* **2007**, *42*, 394-402.
[2]. Dhahagani, K.; Mathan Kumar, S.; Chakkaravarthi, G. , Anitha, K.; Rajesh, J.; Ramu, A.; Rajagopal, G. *Spectrochim. Acta A* **2014**, *117*, 87-94.
[3]. Refat, M. S.; El-Sayed, M. Y.; Adam, A. M. *J. Mol. Struct.* **2013**, *1038*, 62-72.
[4]. Padmaja, M.; Pragathi, J.; Anupama, B.; Gyana, K. C. *E-J. Chem.* **2012**, *9*, 2145-2154.
[5]. Ramadan, A. M.; Ibrahim, M. M.; Shaban, S. Y. *J. Mol. Struct.* **2011**, *1006*, 348-355.
[6]. Viswanathamurthi, P.; Natarajan, K. *Synth. React. Met. Org.* **2006**, *36*, 415-418.
[7]. Yildiz, M.; Dulger, B.; Koyuncu, S. Y. *J. Indian Chem. Soc.* **2004**, *81*, 7-12.
[8]. Lakowicz, J. R. Principles of fluorescence spectroscopy, 3th edition, New York, Springer, 2006.
[9]. Sharma, A.; Schulman, A. G. *Introduction to fluorescence spectroscopy*, New York, John Wiley & Sons, Inc. 1999.
[10]. Basak, S.; Sen, S.; Banerjee, S.; Mitra, S.; Rosair, G.; Rodriguez, M. T. G. *Polyhedron* **2007**, *26*, 5104-5112.
[11]. Omyma, A. M. A.; Samir, M. E.; Doaa, A. A.; Doaa A. N. *Spectrochim. Acta A* **2015**, *144*, 99-106.
[12]. Ali, O. A. M. *Spectrochim. Acta A* **2014,** *121,* 188-195.
[13]. Gupta, K. C.; Abdulkadir, H. K. *J. Macromol. Sci.* A **2007**, *45*, 53-64.
[14]. Pouralimardan, O.; Chamayou, A. C.; Janiak, C.; Hosseini-Monfared, H. *Inorg. Chim. Acta* **2007**, *360*, 1599-1608.
[15]. Nakamoto, K. Infrared and Raman Spectra of Inorganic and Coordination Compounds*,* 5th edition, Wiley Interscience, New York, 1997.
[16]. Spinu, C.; Pleniceanu, M.; Tigae, C. *Turk. J. Chem.* **2008**, *32*, 487-493.
[17]. Lever, A. B. P. *Inorganic electronic spectroscopy*, 2nd edition, Elsevier, New York, 1984.
[18]. Chandra, S.; Gupta, K. *Transition Met. Chem*. **2002**, *27*, 329-332.
[19]. Cotton, F. A.; Wilkinson, G. Advanced Inorganic Chemistry, 4th edition, Wiley, New York, 1980.
[20]. Coats, A. W.; Redfern, J. P. *Nature* **1964**, *20*, 68-69.
[21]. Taakeyama, T.; Quinn, F. X. Thermal Analysis, Fundamentals and Applications to Polymer Science, John Wiley& Sons, Chichester, 1994.
[22]. Frost, A. A.; Pearson, R. G. Kinetic and Mechanisms, 2nd edition, Wiley, New York, 1961.
[23]. Majumder, A.; Rosair, G. M.; Mallick, A.; Chattopadhyay, N.; Mitra, S. *Polyhedron* **2006**, *25*, 1753-1762.
[24]. Liu, Q. X. *Polyhedron* **2009**, *28*, 917-922.
[25]. Omyma, A. M. A.; Samir, M. E.; Maha, R. A.; Abeer, S. S. S. *Spectrochim. Acta* A **2015**, *136*, 654-660.